PROCEEDINGS OF ECOS 2023 - THE 36TH INTERNATIONAL CONFERENCE ON
EFFICIENCY, **C**OST, **O**PTIMIZATION, **S**IMULATION AND ENVIRONMENTAL IMPACT OF ENERGY SYSTEMS
25-30 JUNE, 2023, LAS PALMAS DE GRAN CANARIA, SPAIN

The influence of temperature on internal steam methane reforming in molten carbonate fuel cell

Łukasz Szabłowski*[a]*, Arkadiusz Szczęśniak*[b]*, Aliaksandr Martsinchyk*[c]*,
***Olaf Dybiński*[d]*, Małgorzata Wójcik*[e] *and Jarosław Milewski*[f]**

[a,b,c,d,e,f] *Institute of Heat Engineering, Warsaw University of Technology, Warsaw, Poland*
[a] *lukasz.szablowski@pw.edu.pl*
[b] *arkadiusz.szczesniak@pw.edu.pl*
[c] *aliaksandr.martsinchyk.dokt@pw.edu.pl*
[d] *olaf.dybinski@pw.edu.pl*
[e] *malgorzata.wojcik@pw.edu.pl*
[f] *jaroslaw.milewski@pw.edu.pl*

Abstract:

The article presents the possibility of fueling a molten carbonate fuel cell with a mixture of methane and steam to perform internal steam methane reforming on anode of the fuel cell.

Due to the fact that the optimal operating temperature of MCFC fuel cell is 650°C and the steam reforming process of methane using pure nickel (anode material) as a catalyst takes place at higher temperatures, it seems interesting to test the fuel cell and the reforming process in a non-optimal temperature ranges. The aim of the study is to determine the temperature at which it will be possible to operate of MCFC fuel cell and to carry out the steam reforming of methane. The tested temperature range was from 650°C to 750°C. Testing higher temperatures was not possible due to the limitations associated with the laboratory stand.

The article also presents a mathematical model of a molten carbonate fuel cell operation and a model of the steam reforming process of methane taking place at the anode of this cell.

A reduced order model was used to describe molten carbonate fuel cell operation and kinetic model for methane steam reforming.

Keywords:

Steam methane reforming; SMR; internal reforming; molten carbonate fuel cell; MCFC; influence of temperature; mathematical modelling; nickel catalyst; kinetic model.

1. Introduction

Fuel cells are efficient energy converting systems that allow direct chemical energy conversion into electric energy [1,2]. In United States, European Union countries and Japan, they are widely research and develop as a high efficiency technology. Currently, much attention has been a various types of fuel cells including MCFC and SOFC. The purpose of papers [3,4] is to compare the performance of MCFC and SOFC technology. In comparison with other types of fuel cells as SOFCs, it MCFCs are considered as the most future-proof cells because of its stationary power output, clean and also high-efficiency energy-generating technology [5,6]. Fuel of the MCFC can be biofuels and hydrocarbon fuels that are friendly for environment they don't cause pollution or greenhouse gas emissions. The MCFC system can be classified into the following two types of fuel processing: ER-MCFC and IR-MCFC. In external reforming MCFC (ER-MCFC), a produce hydrogen is at the outside of the MCFC stack.

The stack temperature is only control by convection heat transfer. The ER-MCFC can be require a high rate of cooling gas flow and therefore it is pressurize operation. In this case, a reformer is provided externally of the stack. The second type is an internal reforming MCFC (IR-MCFC). In this case, the reforming reaction is carried out inside the stack by using generated heat. It can be use to directly generate hydrogen in the MCFC stack. These fuel cells are characterized

a high flow rate and they operate under atmospheric conditions. In the IR-MCFC, H2 and CO are reformed by the water-gas shift reaction, CO + H2O ↔ CO2 + H2 and the methane reforming reaction, CH4 + H2O ↔ CO + 3H2. The IR-MCFC can be divided by following types of geometric configurations as Direct Internal Reforming (DIR) and Indirect Internal Reforming (IIR) [7]. In the first case (DIR), produced hydrogen is immediately consumed in the electrocatalytic reaction of the cell. The heat generated by hydrogen oxidation is used in the reforming process. The hydrogen is consumed by a production what it is influence on the equilibrium of reforming process. In IIR, the reforming catalyst is separated from anode compartment. Whereas, in this setup, the hydrogen isn't influenced on the equilibrium of reforming process.

In the literature, one can find several approaches to internal reforming molten carbonate fuel cell systems. A comparison of the performance of internal and external reforming MCFC for varying steam to carbon ratio (S/C) and the current density was referred by Musa et al. [8]. Authors of this publication showed that the more efficiency was in case of S/C ratio equal 2.5 than 4.0 for the IR-MCFC than ER-MCFC and the effect of temperature on the cell voltage [8]. Whereas, Kim et al. [9] studied the temperature and thermal stress distribution and structural stability on thermal effects in external and internal reforming molten carbonate fuel cell systems. Mori et al. [10] have studied the activities of Ni/Li AlO2 using 200 cm3 cell. They have confirmed theoretically and experimentally that methane conversion is increased up to 98% at a steam/methane mole ratio (S/C) range from 1.5 to 3.5 and at temperatures from 600-700°C. Jun et al. [11] carried out a research of intrinsic kinetics for steam methane reforming and reverse water gas shift reaction over Ni/Al2O3 catalyst. Thermodynamic analysis of hydrogen production including SOFC and MCFC system with external and internal reforming was referred by Leal et al. [12]. Other authors like Shikhar et al. [13] compared the IR-SOFC and IR-MCFC system. They found that the IR-MCFC system produces a electric output about a similar efficiency to IR-SOFC and a maximum total efficiency of over 80%. A comparsion of cooling performance and temperature for the Advanced Internal Reforming (AIR) stack and Direct Internal Reforming (DIR) stack of internal reforming type was written by Shinoki and his co-worker [14]. The unsupported nickel powder catalysts as a catalyst in internal or external reforming of SOFC systems were investigated by Rakass, et al. [15]. They have obtained a complete methane conversion at 700°C. The review of the catalytic problems of internal reforming in MCFC and SOFC system was presented in [16]. In these aspects, the activity of cathode and anode to steam methane reforming were evaluated. Camapanari et al. [17] considered an internal and external reforming configuration with combined with a cryogenic CO2 capture section. The best performances was reached by the IR-MCFC with a cryogenic CO2 capture section. A communication of bio-ethanol to produce hydrogen for a IR-MCFC was proposed by Frusteri et al. [18]. As shown that the presence of appropriate amount of oxygen affects a activity and stability of catalyst. Huang et al. [19] presented a comparison of a power output density for the MCFC/TIG and IR-MCFC. The MCFC/TIG hybrid system proved also system about a higher power output density than IR-MCFC.

According to the literature reports, many scientists have recommended a mathematical models to find a solution a problem with MCFC. A short communication about mathematical models of IR-MCFC and ER-MCFC was given by Di Carlo et al. [20]. It was demonstrated that the stack efficiency and electrical power of IR-MCFC was higher in compare to ER-MCFC. Other authors, for example Park et al. [21] used a mathematical modelling to study of temperature distribution, the conversion of methane and the composition of component in the gas flow in the IR-MCFC. The results showed that the differences in temperature distribution are very small in internal and external reforming MCFC. The conversion of methane was more than 99%. Heidebrecht et al. [22] proposed a mathematical model for a countercurrent MCFC with direct internal methane reforming that it enabled the simulation of the gas phase compositions and gas flows, the temperatures in gas and solid phases, the cell voltage as well the current density distribution. However, Lukas et al. [23] used a nonlinear mathematical model of an internal reforming MCFC stack to study in control system applications to fuel cell power plants. A transient model is presented by Heidebrecht et al. [7], who consider the steady state of the system under aspects such temperature distribution, concentrations and velocity profile as well electric efficiency. Mussa et al. [24] successfully modeled the thermodynamic models of IR-MCFC and ER-MCFC in Aspen Plus. Numerical simulations showed that the

IR-MCFC system is more efficient than the ER-MCFC system.

2. Methods and materials

2.1. Reforming model

Chemical reaction speed depends on many factors, among others: catalyst used, temperature, leading reactions.

Most chemical reactions can be written as follows:

$$aA + bB + \ldots \leftrightarrow kK + lL + \ldots, \tag{1}$$

where: a, b, …, k, l, … - number of moles of substrates A, B, … and products K, L, … of the reaction.

The general equation of the chemical reaction (1) is described using stoichiometric coefficients a, b, k, l. Substrates and products are marked here with the capital letters A, B, K and L.

The reaction rate r in a specific, constant and closed volume can be represented by equation (2).

$$-\frac{1}{a}\frac{d[A]}{dt} = -\frac{1}{b}\frac{d[B]}{dt} = \frac{1}{k}\frac{d[K]}{dt} = \frac{1}{l}\frac{d[L]}{dt}, \tag{2}$$

where: [i] is the concentration of component i.

$$r = \frac{d[A]}{dt}, \tag{3}$$

There is a relationship between the degree of reaction, the partial pressures of the reagents and some fixed factors. Rate equation in the system under consideration involves a mass balance equation and reaction rate. The degree of occurrence for components A and B in the reaction can be described as follows [25]:

$$r = k \cdot [A]^a \cdot [B]^b \cdot [X]^x, \tag{4}$$

where: k –reaction rate coefficient, [] – concentrations of reactants, [X] – catalyst impact; b, c, x – coefficients (orders of reaction) considering the type of catalyst, reaction mechanism and its type.

Reaction rate k and temperature are related by the Arrhenius equation:

$$k = A \cdot e^{-\frac{E_a}{R \cdot T}}, \tag{5}$$

where: Ea - activation energy, A - pre-exponential coefficient. The values of these coefficients (A and Ea) depend on the reaction.

More on this subject can be found in [26,27].

2.2. Fuel cell model

MCFC fuel cell is composed of an anode and cathode that are separated by an electrolyte.

An anode and cathode are made of nickel, while an electrolyte is made of lithium carbonate salts that fills up the porous matrix. The description of the mathematical model of the MCFC fuel cell can also be found in [28].

The O_2 and CO_2 partial pressure difference between cathode and anode causes the ion flow between cathode an anode. Cathode reaction is as follows:

$$\frac{1}{2}O_2 + CO_2 + 2e^- \rightarrow CO_3^{2-}, \tag{6}$$

In case of using hydrogen as a fuel, the anode reaction is:

$$H_2 + CO_3^{2-} \rightarrow CO_2 + H_2O + 2e^-, \tag{7}$$

Maximum theoretical voltage is defined as Emax and results from partial pressure difference of O_2 and CO_2 between both sides of fuel cell. Fuel cell electric circuit is simulated as current source with two resistors. In reality, each fuel cell element (cathode, anode and electrolyte) constitutes electrical resistance that was defined as R_1. On the other hand, the electrolyte has both electrical and ionic conductivity that is disadvantage in this case. Electrons flow in the opposite direction to ions. Ions flow is represented by I_2 , while the fuel cell electric resistance is represented by R_2. The current source defines maximum fuel cell voltage, while the resistors represent fuel cell lossess.

Based on Ohm's law and Kirchoff's law, the fuel cell voltage is defined as follows:

$$E_{MCFC} = \frac{E_{max} - \eta_f \cdot i_{max} \cdot r_1}{\frac{r_1}{r_2} \cdot (1 - \eta_f) + 1}, \tag{8}$$

where: E_{max}– maximum theoretical voltage, η_f – fuel utilization factor, i_{max} – maximum current density, r_1 – specific ionic resistance, r_2 – specific electric resistance.

Equation (9) uses parameters of current and resistance in reference to the total active area of fuel cell:

$$i = \frac{I}{A} \tag{9}$$

$$\mathrm{r = R \cdot a}, \tag{10}$$

where: A – area of the fuel cell.

2.2.1 Maximum voltage E_{max}

Fuel cell produces electricity and heat staying in constant temperature, what makes the process isothermal. In this case, maximum work performed may be described with equation (11):

$$L_{\max} = M \cdot R \cdot T \cdot \ln \frac{p_{in}}{p_{out}}, \tag{11}$$

where: M – amount of moles taking part in work performed; p – partial pressure.

It is necessary to specify amount of moles taking part in the process and difference between partial pressure on both sides (cathode and anode stream) before maximum work performed may be determined. In case of MCFC, work is performed by O_2 and CO_2 flowing through cathode side to the anode side. Maximum power generated by fuel cell depends on the flow of ions through electrolyte, which are transported by O_2 and CO_2 particles. Using Faraday's law, it is possible to describe current in the fuel cell with an equation:

$$\mathrm{I = n \cdot M \cdot F}, \tag{12}$$

where: n – electric load transported by carbonate ions, M – amount of moles transported in time period, F – Faraday's constant

In case of MCFC, single CO_3^{2-} element, during movement from cathode to anode is able to carry 4 electrons, thus parameter "n" equals 4. Summarizing the above considerations, Nerst equation compatible for MCFC analysis can be presented:

$$E_{\max} = \frac{R \cdot T}{4F} \ln \frac{p_{O_2,cathode} \cdot p^2_{CO_2.cathode}}{p_{O_2,anode} \cdot p^2_{CO_2.anode}}, \tag{13}$$

2.2.2 Maximum current density i_{max}

Maximum current generated by single cell depends on the amount of fuel and/or oxidizer.

In case where 100% of the fuel delivered to the fuel cell is utilized, maximum current density is achieved. However, maximum current depends also on the total active area of the fuel cell. The larger fuel cell area, the bigger current can flow. The maximum current is however given usually as I/cm^2, thus this value is called current density and described as I_{max}.

$$i_{\max} = \frac{2F \cdot n_{H_2,equivalent}}{A}, \tag{14}$$

where: $n_{H2,equivalent}$ – defined hydrogen flow.

2.2.3 Ionic resistance r_1

Ionic resistance is a function of electrolyte thickness and temperature in each layer of the MCFC. It is described with equation:

$$r_1 = \sum_i^l r_{1,anode,i} + \sum_j^m r_{1,electrolyte,j} + \sum_k^n r_{1,cathode,k}, \tag{15}$$

Fuel cell matrix is soaked with electrolyte. Ionic resistance of each layer of the fuel cell can be described with equation:

$$r_{1,electrolyte} = \frac{\delta_{electrolyte}}{\sigma_{1,electrolyte}}, \tag{16}$$

where: δ – electrolyte layer thickness; σ_1 – ionic conductance.

In the literature there are presented different methods for defining of ionic conductance of the electrolyte. For example, Kai Sundmacher et al. [29] suggested the following definition:

$$\sigma_1 = \frac{1}{\beta_1} e^{\frac{\beta_2}{T}}, \tag{17}$$

where: β_1, β_2 – empirical parameters depending on the material of which the electrolyte is made of (for example: $\beta_1 = 3.34 \times 10^{-4}$ S/m, $\beta_2 = 1.03 \times 10^4$ K).

Carbonates which are utilized for production of the electrolyte for the MCFC have good ionic conductance in high temperatures. Even though in the literature there are no strict dependences between temperature and ionic resistances presented, there are papers presenting equations for this definition [30]. Thus, basing on the literature, ionic conductance of the electrolyte can be described by:

$$\sigma = \sigma_0 \cdot e^{\frac{-E_{act}}{R \cdot T}}, \tag{18}$$

where: : σ_0 [S/cm]; E_{act} [kJ/mol] – coefficients related to the material of which the electrolyte is made of [4].

2.2.4 Electrical resistance r_2

In addition to ionic conductivity, MCFC cells are also characterized by electric conductivity. Electric conductivity as well as air and carbon dioxide leaks reduce the maximum possible cell voltage, but the more loaded the cell, the less impact these factors is. Electrical conductivity can be determined from the equations presented above. When the fuel cell does not produce electricity, the fuel utilization factor is equal to zero $\eta_f = 0$, so using equation 8 we get:

$$E_{OCV} = \frac{E_{\max}}{\frac{r_1}{r_2} + 1} \tag{19}$$

Electrical resistance can be determined in the same way as ionic resistance:

$$r_2 = \frac{\delta}{\sigma_2} \tag{20}$$

Using equations 20 and 19, it is possible to determine the electronic conductivity in the following form:

$$\sigma_2 = \delta \cdot \frac{E_{max} - E_{OCV}}{r_1 \cdot E_{OCV}}, \tag{21}$$

3. Experimental setup

T The tests were carried out on a laboratory stand of the Institute of Heat Engineering of the Warsaw University of Technology. This stand allows for the automated measurement of process parameters. It is possible to set the temperature of the cell and the flows of various gases to power the cell. The laboratory stand is shown in Fig. 1.

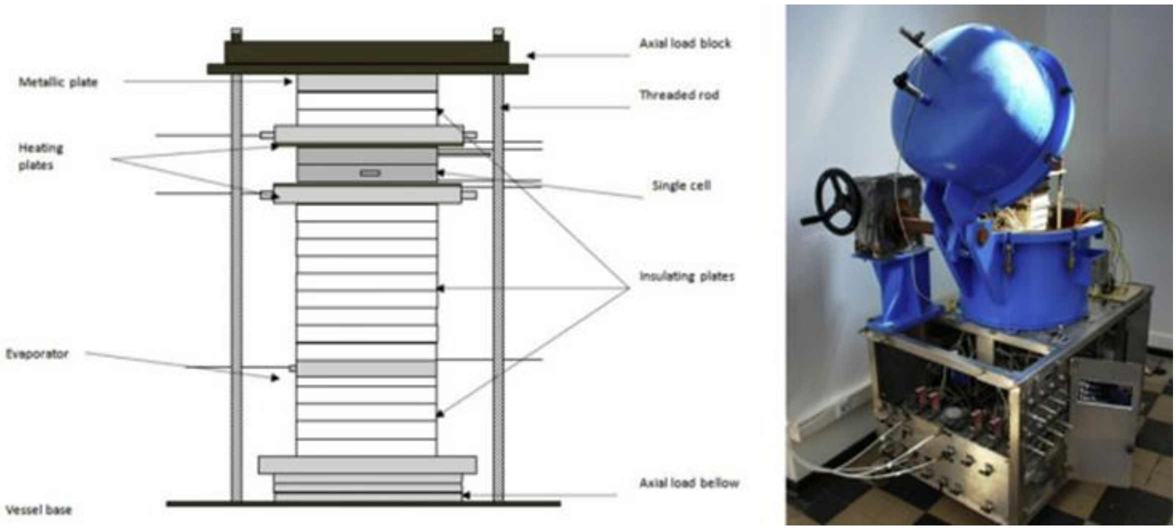

Figure. 1. Laboratory stand: stack layout (left side), general view (right side) for testing high-temperature fuel cells owned by the Institute of Heat Engineering of Warsaw University of Technology.

The experimental stand consists of an integrated electronic device equipped with control and regulation elements (thermocouples, thermostats, electric heaters, mass flow regulators, current and voltage measurements and regulators) all controlled by software created in the LabView environment. This stand is connected to the following media: hydrogen, CO_2, N_2 and compressed air. The additional elements as methane delivered from a bottle, and water delivered via a peristaltic pump were required for the experiments. Water mixed with methane was delivered through the anode channel filled with the catalyst, and was heated to the required temperature by electric heaters, which also kept the temperature of the fuel cell at the required level. CO_2 and air were delivered to the cathode channel, and heated to the required temperature. The fuel cell used in the experiments was between the gas delivery manifolds.

4. Results

The results section is divided into three subsections where the following are discussed: the results of experimental research, the post mortem analysis and the results of the model.

4.1 Experimental research

Figure 2 shows the polarization curves for the MCFC fuel cell, whose anode is fed with different gas compositions, in order to study the performance of this cell when fueled with a mixture of methane and steam. Reference tests were also carried out while working on hydrogen and on pure methane.

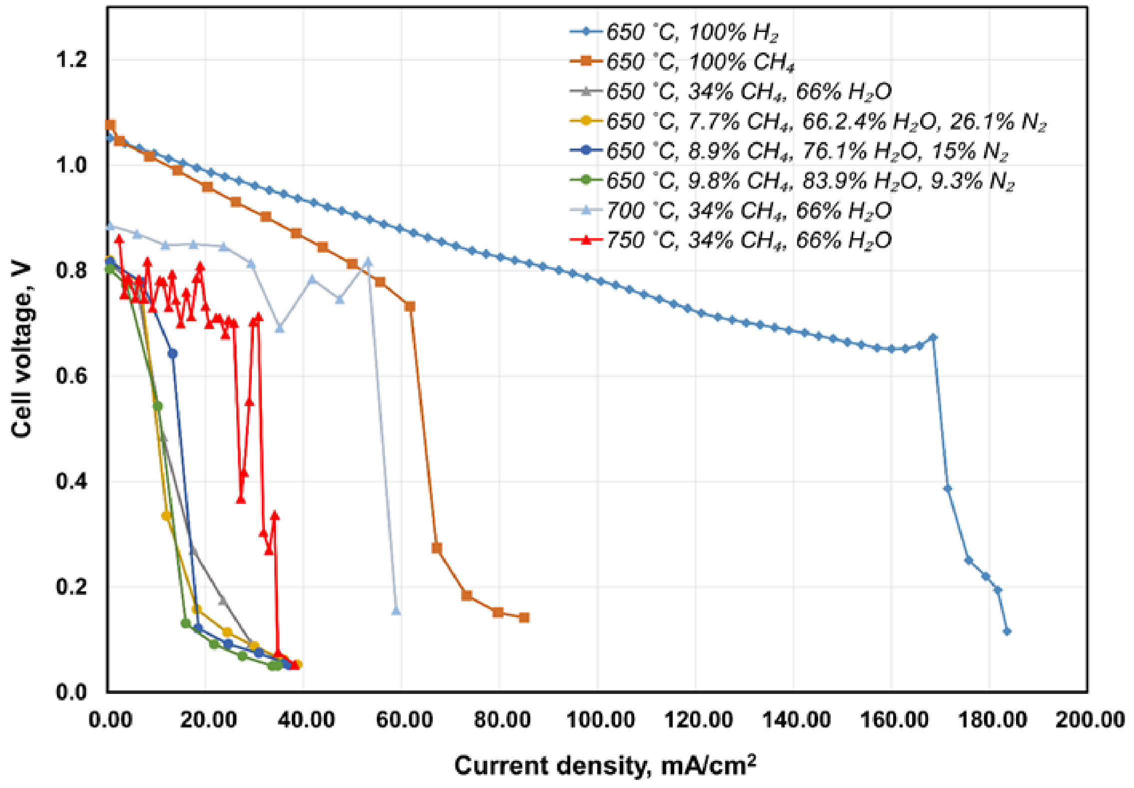

Figure. 2. Electrochemical characteristic (i-E) of MCFC on pure H2 compared under different operation parameters.

In turn, Figure 3 shows the power densities as a function of the current density for the same experiments.

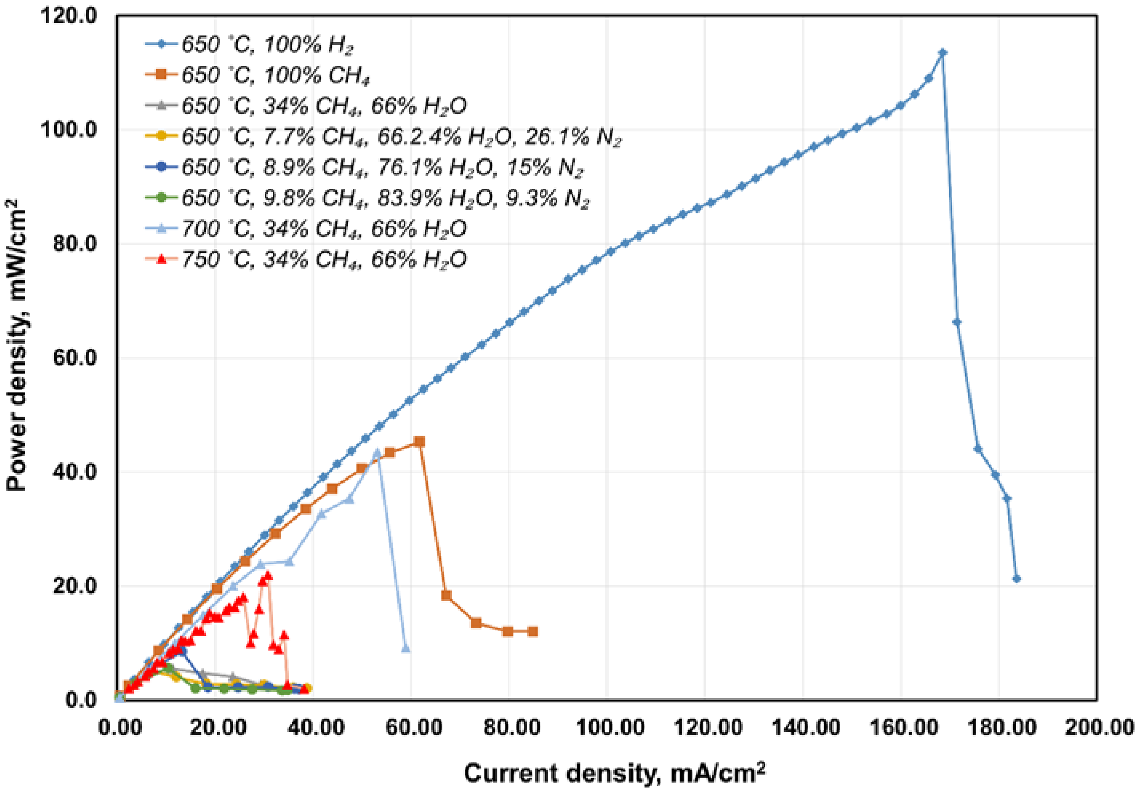

Figure. 3. Power density characteristics (P-i) of MCFC on pure H_2 compared under different operation parameters.

Both of these Figures clearly show that the best results were obtained for a cell operating on pure hydrogen. Interestingly, the cell worked better on pure methane than in the case of a mixture of methane and steam. In the case of work on a mixture of methane and steam (which is supposed to result in steam reforming of methane at the anode of the cell), the best results were obtained for 700°C and a methane to water ratio of 1:2. One would expect that the results should improve with increasing temperature (because it accelerates the methane steam reforming reaction), but at 750°C the results are weaker than at 700°C. This can be explained by the fact that at 750°C the MCFC fuel cell itself begins to operate less well.

4.1 Post-mortem analysis

The results of the post mortem analysis of the cell are shown in the Figure 4.

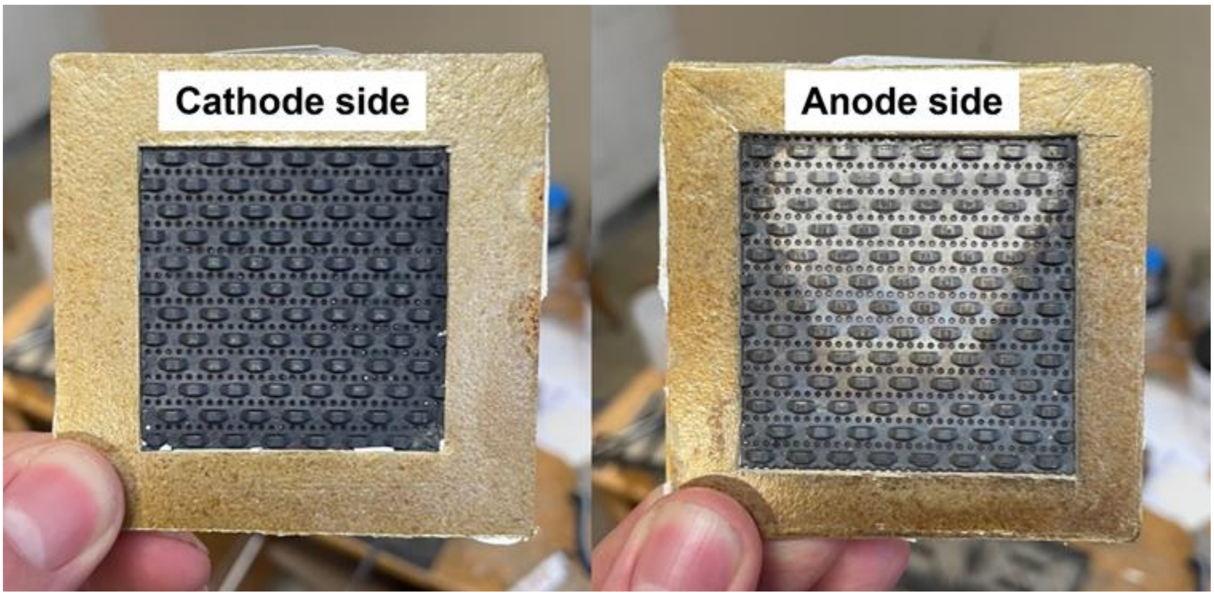

Figure. 4. Current collector of cathodic and anodic sides of MCFC after disassembly.

The photos do not show carbon deposition on the anode current collector. There are also no substances on the current collectors that could disturb the flow of gases.

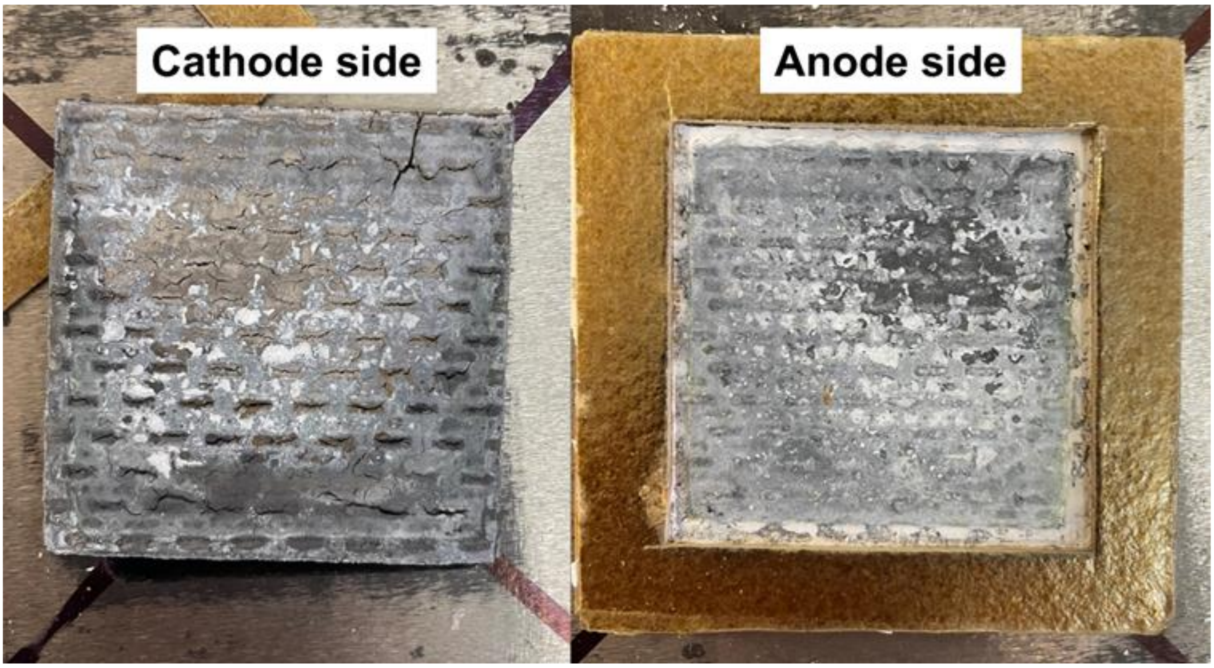

Figure. 5. Anode and cathode electrodes of MCFC after disassembly.

Figure 5 shows the cathode and anode after shut down of the cell. Minor cracks can be seen on the cathode, however, no gas leaks between the anode and cathode sides were found during normal operation of the cell.

4.3 Results of the mathematical model

The next step of the research was comparison of simulation results with the experimental data. Detailed model description is presented in the section "Methods and materials". The model was verified for 3 curves (I) operation on CH4 only, (II) operation on 34:66 CH_4:H_2O at temperature 700°C and (**III**) 750°C.

In the case of a mathematical model, not all curves were suitable for modelling. Some of them had too short a curve associated with the normal operation of the cell.

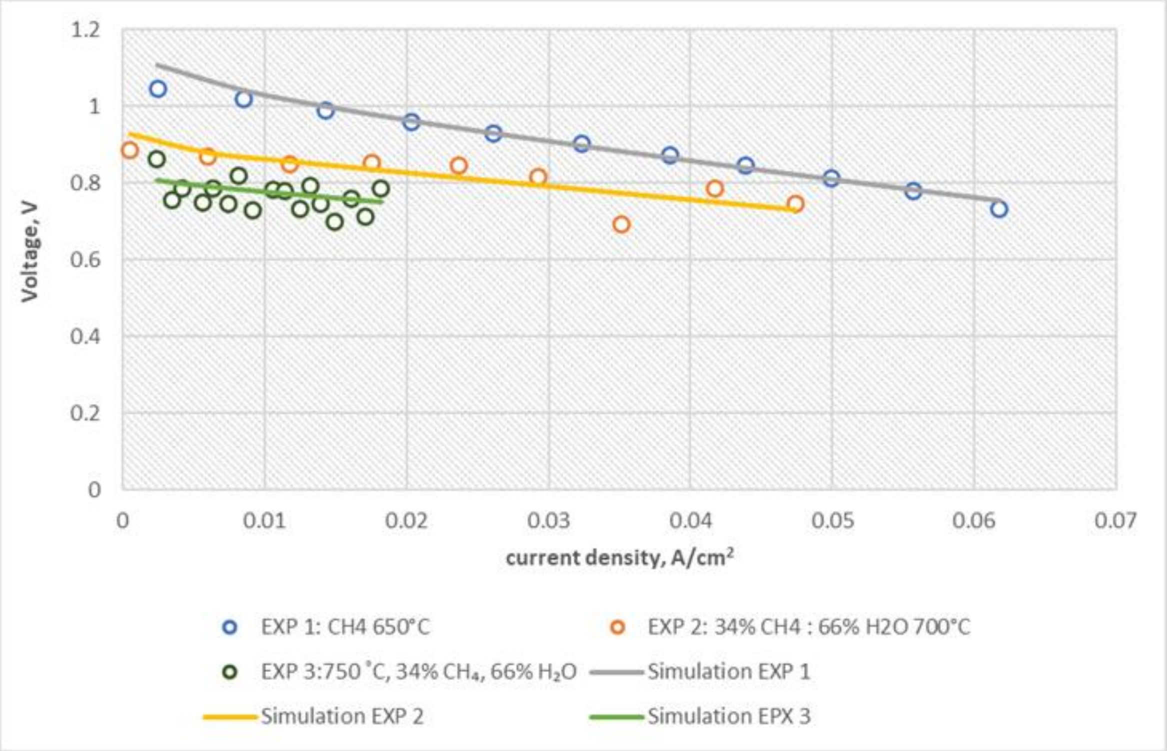

Figure. 6. The comparison of experimental data and simulation results.

The comparison of experimental data is shown in Figure 6. The average relative error is ca. 1%, while the maximum relative error reaches almost 10%. The chart indicates the model shows good prediction of experimental data, thus it could be used for examination of cell performance when operating with a mixture of methane and steam.

5. Conclusions

The tested temperature range was from 650°C to 750°C. Testing higher temperatures was not possible due to the limitations associated with the laboratory stand. Due to the fact that the electrolyte of the MCFC cell evaporates quite intensively at higher temperatures, such a test would also make no sense from the point of view of the cell's lifetime.

The best results were obtained for a cell operating on pure hydrogen. Interestingly, the cell worked better on pure methane than in the case of a mixture of methane and steam. In the case of work on a mixture of methane and steam (which is supposed to result in steam reforming of methane at the anode of the cell), the best results were obtained for 700°C and a methane to water ratio of 1:2. One would expect that the results should improve with increasing temperature, but at 750°C the results are weaker than at 700°C. This can be explained by the fact that at 750°C the MCFC fuel cell itself begins to operate less well.

This means that the model shows good prediction of experimental data, thus it could be used for examination of cell performance when operating with a mixture of methane and steam.

Acknowledgments

This research was funded by the National Science Center, Poland (Grant number 2020/39/D/ST8/02021).

References

[1] Larminie J, Dicks A. Fuel cell systems explained: Second edition. 2013. https://doi.org/10.1002/9781118878330.

[2] NETL. Seventh Edition Fuel Cell Handbook. vol. 7 Edition. 2004.

[3] Tomczyk P. MCFC versus other fuel cells-Characteristics, technologies and prospects. J Power Sources 2006;160. https://doi.org/10.1016/j.jpowsour.2006.04.071.

[4] Karvountzi GC, Price CM, Duby PF. Comparison of molten carbonate and solid oxide fuel cells for integration in a hybrid system for cogeneration or tri-generation. Am. Soc. Mech. Eng. Adv. Energy Syst. Div. AES, vol. 44, 2004. https://doi.org/10.1115/IMECE2004-59927.

[5] Pesch HJ. Molten Carbonate Fuel Cells Edited by Kai Sundmacher , Achim Joachim F . Berndt , and Gerhard Huppmann. Fuel Cells 2007.

[6] Antolini E. The stability of molten carbonate fuel cell electrodes: A review of recent improvements. Appl Energy 2011;88:4274–93. https://doi.org/10.1016/J.APENERGY.2011.07.009.

[7] Heidebrecht P, Sundmacher K. Molten carbonate fuel cell (MCFC) with internal reforming: model-based analysis of cell dynamics. Chem Eng Sci 2003;58. https://doi.org/10.1016/S0009-2509(02)00644-9.

[8] Musa A, Steeman H, De Paepe M. The effect of operating temperature on the performance of molten carbonate fuel cell systems. 16th World Hydrog Energy Conf 2006, WHEC 2006 2006;2:1532–43.

[9] Kim YJ, Lee MC. Comparison of thermal performances of external and internal reforming molten carbonate fuel cells using numerical analyses. Int J Hydrogen Energy 2017;42. https://doi.org/10.1016/j.ijhydene.2016.10.165.

[10] Mori T, Higashiyama K, Yoshioka S, Kobayashi T, Itoh S. Steam Reforming Reaction of Methane in Internally-Reformed Molten Carbonate Fuel Cell. J Electrochem Soc 1989;136. https://doi.org/10.1149/1.2097272.

[11] Jun CS, Park S, Kim YS, Lee TW. The characterization of catalyst for Internal Reforming Molten Carbonate Fuel Cell. AIChE Annu. Meet. Conf. Proc., 2008.

[12] Leal EM, Brouwer J. A thermodynamic analysis of electricity and hydrogen CO-production using a solid oxide fuel cell. Proc. 3rd Int. Conf. Fuel Cell Sci. Eng. Technol. 2005, 2005. https://doi.org/10.1115/fuelcell2005-74136.

[13] Shikhar U, Hemmes K, Woudstra T. Exploring the Possibility of Using Molten Carbonate Fuel Cell for the Flexible Coproduction of Hydrogen and Power. Front Energy Res 2021;9. https://doi.org/10.3389/fenrg.2021.656490.

[14] Shinoki T, Matsumura M, Sasaki A. Development of an Internal Reforming Molten Carbonate Fuel Cell Stack. IEEE Trans Energy Convers 1995;10. https://doi.org/10.1109/60.475845.

[15] Rakass S, Oudghiri-Hassani H, Rowntree P, Abatzoglou N. Steam reforming of methane over unsupported nickel catalysts. J Power Sources 2006;158. https://doi.org/10.1016/j.jpowsour.2005.09.019.

[16] Clarke SH, Dicks AL, Pointon K, Smith TA, Swann A. Catalytic aspects of the steam reforming of hydrocarbons in internal reforming fuel cells. Catal Today 1997;38. https://doi.org/10.1016/S0920-5861(97)00052-7.

[17] Campanari S, Manzolini G, Chiesa P. Using MCFC for high efficiency CO2 capture from natural gas combined cycles: Comparison of internal and external reforming. Appl Energy 2013. https://doi.org/10.1016/j.apenergy.2013.01.045.

[18] Frusteri F, Freni S. Bio-ethanol, a suitable fuel to produce hydrogen for a molten carbonate fuel cell. J Power Sources 2007;173. https://doi.org/10.1016/j.jpowsour.2007.04.065.

[19] Huang C, Pan Y, Wang Y, Su G, Chen J. An efficient hybrid system using a thermionic generator to harvest waste heat from a reforming molten carbonate fuel cell. Energy Convers Manag 2016;121. https://doi.org/10.1016/j.enconman.2016.05.028.

[20] Di Carlo A, Bocci E, Dell'Era A. Comparison by the use of numerical simulation of a MCFC-IR and a MCFC-ER when used with syngas obtained by atmospheric pressure biomass gasification. Int J Hydrogen Energy 2011;36. https://doi.org/10.1016/j.ijhydene.2011.01.095.

[21] Park HK, Lee YR, Kim MH, Chung GY, Nam SW, Hong SA, et al. Studies of the effects of the reformer in an internal-reforming molten carbonate fuel cell by mathematical modeling. J Power Sources 2002;104. https://doi.org/10.1016/S0378-7753(01)00912-0.

[22] Heidebrecht P, Sundmacher K. Dynamic Modeling and Simulation of a Countercurrent Molten Carbonate Fuel Cell (MCFC) with Internal Reforming. Fuel Cells 2002;2. https://doi.org/10.1002/fuce.200290016.

[23] Lukas MD, Lee KY, Ghezel-Ayagh H. Development of a stack simulation model for control study on direct reforming molten carbonate fuel cell power plant. IEEE Trans Energy Convers 1999;14. https://doi.org/10.1109/60.815119.

[24] Musa A, Steeman HJ, De Paepe M. Performance of internal and external reforming molten carbonate fuel cell systems. J Fuel Cell Sci Technol 2007;4. https://doi.org/10.1115/1.2393306.

[25] Young DC. Computational chemistry: a practical guide for applying techniques to real world problems.

New York: Wiley; 2001.

[26] Szablowski L, Kupecki J, Milewski J, Motylinski K. Kinetic model of a plate fin heat exchanger with catalytic coating as a steam reformer of methane, biogas, and dimethyl ether. Int J Energy Res 2019;43. https://doi.org/10.1002/er.4465.

[27] Szablowski L, Dybinski O, Szczesniak A, Milewski J. Mathematical Model of Steam Reforming in the Anode Channel of a Molten Carbonate Fuel Cell. Energies 2022;15. https://doi.org/10.3390/en15020608.

[28] Milewski J, Wołowicz M, Miller A, Bernat R. A reduced order model of molten carbonate fuel cell: A proposal. Int J Hydrogen Energy 2013;38:11565–75.

[29] Sundmacher K, Kienle A, Pesch HJ, Berndt JF, Huppmann G. Molten Carbonate Fuel Cells: Modeling, Analysis, Simulation, and Control. 2007. https://doi.org/10.1002/9783527611324.

[30] Morita H, Komoda M, Mugikura Y, Izaki Y, Watanabe T, Masuda Y, et al. Performance analysis of molten carbonate fuel cell using a Li/Na electrolyte. J Power Sources 2002;112. https://doi.org/10.1016/S0378-7753(02)00468-8.